HIV-1 Vpu protein forms stable oligomers in aqueous solution via its transmembrane domain self-association

Saman Majeed[#][a], Lan Dang[#][b], Md Majharul Islam[a], Olamide Ishola[a], Peter P. Borbat[c], Steven J. Ludtke*[d], Elka R. Georgieva*[e][f]

[a]Department of Chemistry and Biochemistry, Texas Tech University, Lubbock, TX 79409, USA

[b]Graduate Program in Quantitative and Computational Biosciences, Graduate School of Biomedical Sciences at Baylor College of Medicine, Houston, Texas, USA

[c]Department of Chemistry and Chemical Biology and ACERT, Cornell University, Ithaca, NY 14853, USA

[d]Department of Biochemistry and Molecular Biology, Baylor College of Medicine, Houston, TX 77030, USA, correspondence e-mail: sludtke@bcm.edu

[e]Department of Chemistry and Biochemistry, Texas Tech University, Lubbock, TX 79409, USA, correspondence e-mail: elgeorgi@ttu.edu

[f]Center for Membrane Protein Research, TTU Health Science Center, Lubbock, TX 79430, USA

[#]Equal contribution

Supporting information for this article is given via a link to this document.

Abstract: We study the structure of the HIV-1 encoded protein Vpu, which fulfils important roles for the virus functions. To date, Vpu has been considered exclusively a single-pass membrane protein. However, our studies revealed that this protein forms stable oligomers in aqueous solution with currently unknown physiological role. Therefore, the detailed characterization of the structure of these oligomers might shed light on possible function, but will also contribute valuable knowledge to the biochemical and biophysical properties of membrane proteins. Here, we report on our findings about the organization of soluble Vpu oligomers. We utilized protein engineering, size exclusion chromatography, single particle cryoEM and electron paramagnetic resonance (EPR) spectroscopy. We found that Vpu oligomerizes via its N-terminal transmembrane domain, but the subsequent C-terminal region is important for oligomer stability. CryoEM analyses suggest that the oligomeric state most likely is a hexamer or exists in hexamer-to-heptamer equilibrium. Both cryoEM and EPR suggest that, within the oligomer, the distant C-terminal region of Vpu is highly flexible.

Introduction

The HIV-1 encoded Vpu protein fulfils important functions aiding virus adaptation and proliferation.[1] Despite its small size of about 80 amino acids (aa), the protein has a multi-domain organization and participates in diverse interactions with cellular components. It consists of a short soluble N-terminus followed by what is believed a transmembrane Helix 1 (TM), and two soluble helices Helix 2 and Helix 3 in the C-terminal domain (Figure 1).[1e, 2] The current knowledge is that Vpu spans the membrane bilayer through its TM Helix 1; it resides and functions in the plasma membrane (PM) and endomembranes of infected cell; it forms a homo-oligomer (presumably a pentamer) in the membranes of Golgi and

intracellular vesicles, but not in the endoplasmic reticulum (ER).[3] Monomeric Vpu associates with human tetherin (BST2 protein) in PM via TM Helix 1 forming a Vpu-tetherin complex, leading to enhancement of tetherin ubiquitination and its trafficking for degradation.[4] Therefore, apparently when associated with cellular membranes, this protein exists in several functional quaternary structures. Recently, we found that in addition to membrane-bound self-association, full-length (FL) Vpu also forms homo-oligomers in aqueous solution outside a lipid/hydrophobic environment.[5]

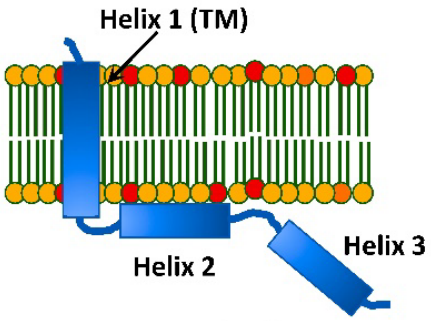

Figure 1. A cartoon representation of the topology of HIV-1 Vpu in lipid membranes: Vpu traverses the membrane via its hydrophobic Helix 1 (TM helix). Helix 2 is membrane-associated; however, other model of Helix 2 not making a contact with the membrane surface was also proposed.

Although, such Vpu self-association has been reported before,[3a] we have recently characterized these oligomers in more detail by using a range of biochemical and biophysical techniques, which are analytical size exclusion chromatography (SEC), negative staining electron microscopy (nsEM) and electron paramagnetic resonance (EPR) spectroscopy, revealing that they are rather stable and uniform at protein concentrations of and above 5 μM.[5] This was an interesting result, given that the prevailing opinion is that Vpu is exclusively a transmembrane protein. Furthermore, a previous study found that soluble Vpu oligomers form even upon the expression of this protein *in vivo*,[3d] which along with our findings brings the question about the possible physiological role of the soluble Vpu form. It could be that the protein is even more functionally versatile than what is currently known about its physiological roles, because of its capacity to transition from soluble to membrane-bound form. Several other unconventional transmembrane proteins from eukaryotic and prokaryotic organisms are known to exists and function in both soluble and membrane-bound states, e.g., the members of Bcl-2 family,[6] bacterial toxins,[7] etc., suggesting that this could be the case for Vpu as well.

To advance the understanding of the soluble Vpu oligomers we aimed at characterizing them in greater detail by using the MBP-Vpu construct developed previously[5] and studying it by cryoEM in combination with SEC and also by continuous wave electron paramagnetic resonance (CW EPR) and double electron-electron resonance (DEER) spectroscopy. The acquired data confirmed with high confidence that in aqueous environment Vpu forms stable oligomers.

Results and Discussion

The Vpu soluble oligomers are a result of Helix 1 (TM) self-association

To establish with certainty which region of Vpu contributes to its oligomerization in solution, in addition to MBP-FL Vpu, we produced two truncated versions of Vpu that are MBP-VpuΔh3 and MBP-VpuΔh2h3 (with deletions of either Helix 3 or both Helices 2 and 3). We studied these protein versions with SEC and found that all MBP-Vpu variants elute as oligomers of close molecular weight (Figure 2). MBP-Vpu oligomers were formed even when both

Helices 2 and 3 were deleted, although the corresponding elution peak at 8.5 – 12 ml was broader than the elution peaks of MBP-FL Vpu and MBP-VpuΔh3. The estimated FWHM for these peaks were 0.74, 0.85 and 1.5 (in ml), respectively, for the FL Vpu, VpuΔh3, and VpuΔh2h3. The observed elution peak broadening for Vpu lacking both Helix 2 and Helix 3 indicates that just Helix 1 is insufficient for stabilizing the Vpu oligomers, leading to increased heterogeneity in the oligomeric order. Still, no complete oligomer disassembly occurs, as the intensity of the SEC elution peak at 16 – 18 ml remains unchanged (Figure 2). On the other hand, a little if any difference was observed in the SEC profiles of MBP-FL Vpu and MBP-VpuΔh3 suggesting the essential role of protein region comprising Helices 1 and 2 in Vpu self-assocation and oligomer stabilization, which is in agreement with what was proposed for Vpu oligomer in lipid environment.[3c]

cryoEM provides a solid evidence about the formation of stable soluble MBP-FL Vpu oligomers

In a previous study, we utilized nsEM to observe stable soluble oligomers of MBP-Vpu.[5] These oligomers were typically formed at protein concentrations exceeding 5 μM, which indicated that cooperative mechanisms may have contributed to this process. MBP-FL Vpu oligomers were imaged using cryoEM to confirm that the well-defined soluble oligomers observed by nsEM are reproducible under cryoEM conditions that utilize fast freezing of the sample. The cryoEM freezing process occurs on the timescale, which is too fast for water ice to form and grow and for kinetically slow processes, such as oligomer disassembly, to materialize,[8] thereby preserving the native protein state.

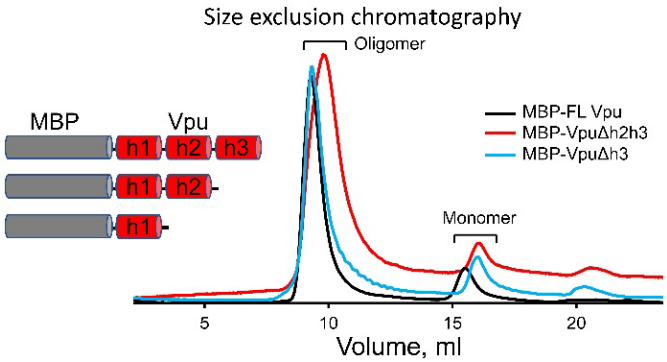

Figure 2. Results from SEC on MBP-Vpu protein in buffered aqueous solution. The SEC results demonstrate that all the MBP-FL Vpu, MBP-VpuΔh3 and MBP-VpuΔh2h3 constructs form oligomers, as they elute predominantly at about 8.5 – 12 ml (depending on the construct) and only small fraction elutes as monomers corresponding to the peak at 16 – 18 ml. The protein concentration was 15 μM for all the three constructs.

To perform structural analysis by single-particle cryoEM, purified MBP-FL Vpu protein was used. The oligomerization of MBP-FL Vpu in buffer solution was confirmed by SEC (Figure 2) prior to cryoEM imaging. CryoEM data collected in the present study had sufficient contrast to enable clear visualization of oligomeric proteins in the raw micrographs (Figure 3A). We collected a data set of 14,657 putative oligomeric particle images, sufficient for structural analysis. A representative micrograph containing MBP-Vpu oligomers, and reference-free 2D class averages are shown in Figures 3A and 3B, respectively. The micrograph exhibits mostly oligomeric assemblies similar to those previously observed in nsEM,[5] but a small fraction of lower order oligomers and possibly monomers were also present. Notably, the majority of the self-associated protein particles were of a visually similar size, and only small fraction of non-specific larger aggregates could be found. When further analyzed, the visibly uniform particles readily group into unsupervised classes of a similar size implying a self-consistent quaternary structure of size-limited protein oligomers.

To confirm whether the class-averages represent different views of a single 3-D quaternary structure or represent multiple states, we conducted de-novo reconstructions using EMAN2,[9] performing several cross-validations and classification attempts. The analysis produced two self-consistent 3-D structures at low resolution (~25 Å), representing different populations of the observed particles. Out of a total of 14,657 particles, about 80% were associated with one larger-size structure (shown in Figure 3C) with several low-intensity features, whereas the remaining about 20% of the particles correspond to a similar, but slightly smaller-size structure (Figure 3D). The densities populating the centers of the structures in Figures 3C and 3D, presumably correspond to the Vpu TM oligomer core (shown in Figure 3D). The small densities observed outside of the structures, more visible in Figure 3D (encircled in yellow) could be attributed to a particular arrangement of the distant Vpu C-terminal helices. We made attempts to further classify the particles or characterize the remaining variability in the system not accounted for in the two classes by using a deep-learning Gaussian Mixture Model (GMM) approach.[10] However, this effort did not yield useful insights beyond confirming the overall positioning of the major densities in both structures with the persisting variability at the level of the ~25 Å resolution. The high monomer flexibility due to MBP-Vpu linker and currently unknown Vpu folding state in the soluble form, and variations in the oligomeric order majorly contribute to the low structural resolution.

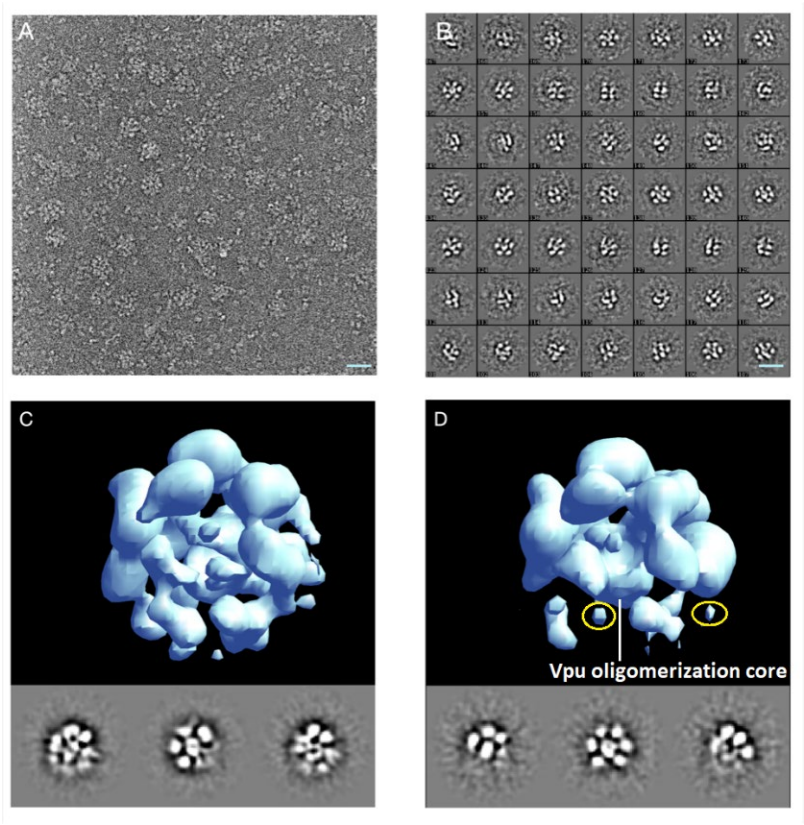

Figure 3. Single particle cryoEM analysis of MBP-FL Vpu soluble oligomers. (A) A micrograph showing representative oligomers and dissociated monomers; (B) representative unsupervised 2D class averages from 14,657 particles; (C-D) single-particle reconstruction of the two identified particle populations with 11,541 (C) and 2815 (D) respectively. The presumably Vpu oligomeric core and low densities from the distant Vpu C-terminus are shown in (D) with white line and yellow circles, respectively. The scale bar is 20nm.

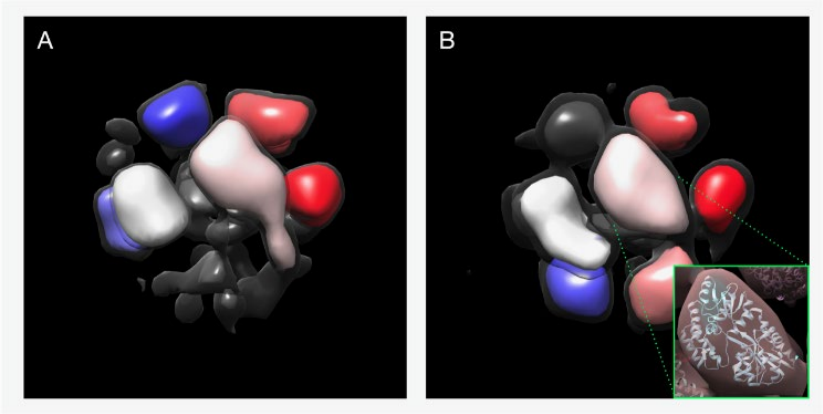

Figure 4. (A-B) Maps of the two oligomeric states shown in Figure 3 C-D respectively, colored to indicate regions where MPB could be docked. Views are from different angle than those in Figure 3. A lower isosurface threshold presented in transparent gray shows the lower-density connections in the reconstruction. The inset shows an MBP molecule (PDB: 1PEB) docked into the pink density region of the 3D model as a representative example.

The obtained structural models of MBP-Vpu do not provide sufficient structural resolution for further accurate docking of the Vpu oligomeric core; at this resolution and with limited constraints on the isosurface threshold level, it can only be generally placed within the total structure density. On the other hand, due to larger size and greater stability, the densities of MBP in the 3-D structures, could be modeled through docking to estimate the number (N) of MBP moieties, hence the number of MBP-Vpu protomers. We were able to dock the MBP moieties into six MBP-sized domains in both CryoEM maps. The docked MBP moieties in Figure 4 are colored, whereas the remaining densities, shown in gray should account for the Vpu oligomerization core. The gray density in the structure shown in Figure 4A is more prominent, so it may well be that it can accommodate a seventh MBP-Vpu protomer, which might imply heptamer-to-hexamer oligomer equilibrium.

Protein spin labeling and EPR spectroscopy confirm that the distant C-teminus of Vpu is highly dynamic

Before undertaking full-fledged multi-site spin labeling EPR experiments to map protein dynamics and solve spatial organization of monomers in the Vpu oligomer, we limited this task to using two carefully selected spin-labeled sites in an effort-saving approach. We reused the generated previously single cysteine mutant Q36C[5] in the linker at the beginning of Helix 2 N-terminal side and added new labeling site N55C in the linker connecting Helix 2 to Helix 3 (Figure 5A).

The broad CW EPR spectrum recorded for spin-labeled Q36C mutant (Figure 5B) reinforced the previous conclusion that this protein region has restricted motional dynamics.[5] This is in line with the SEC results showing that the linker connecting Helices 1 and 2 play a role in Vpu soluble oligomer stabilization. This may require specific structural arrangement of the protein region containing residue 36. Could be that this linker is ordered, possibly in contact with the oligomer-forming Helices 1. On the other hand, the CW EPR spectrum for the spin-labeled residue N55C has narrow lines (Figure 5B), indicating that this protein region is highly mobile and possibly unstructured,[11] in agreement with the structures of monomeric Vpu C-terminal (Figure 5A).[12] However, a minor population of protein conformation with restricted motional dynamics at this site contributing broad low-intensity lines to the EPR spectrum of this spin-labeled residue while cannot be ruled out was not immediately apparent in the signal dominated by the high-intensity lines of the predominant conformation.

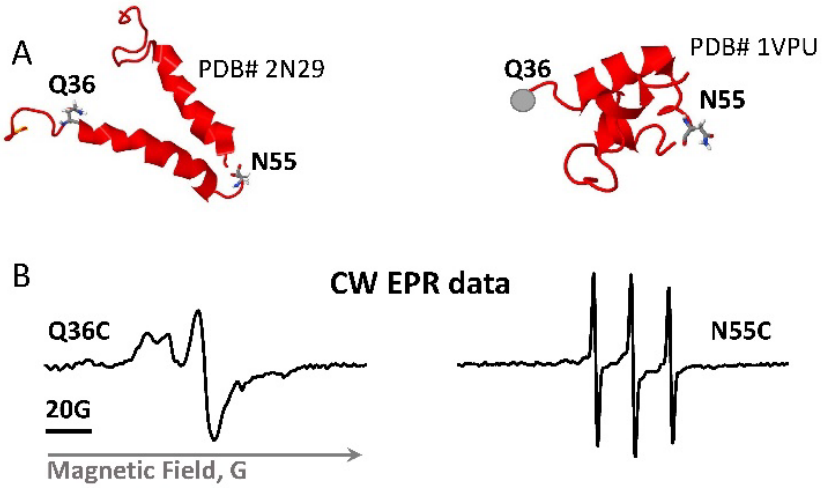

Figure 5. Vpu spin labeling and CW EPR results. (A) Shown are two NMR structures of the soluble C-terminal domain of the Vpu protein with the residues mutated to cysteines and spin-labeled. The residue Q36C is located at the beginning of amphipathic Helix 2, residue N55C is in highly dynamic loop connecting Helices 2 and 3. (B) EPR spectra of spin-labeled residues Q36C and N55C show very different mobility of spin labels at these sites.

The pulse EPR (DEER) data for the Q36C mutants were already recorder and published.[5] It was of more interest to conduct DEER distance measurement for the newly spin-labeled residue N55C, probing conformations of this protein region. For the DEER measurements of this mutant, we used partial or full solvent deuteration by substituting H_2O for D_2O and glycerol for glycerol-d_8 in the buffer aiming to increase the signals and extend the upper range of measurable distances at least for more water exposed spin-labeled sites due to increased spin label phase memory relaxation time, T_m.[13]

Unlike Q36C,[5] the residue N55C is favorable to spin labeling. Long T_m's and larger primary echo amplitude compared to Q36C (Supporting Information) show that this residue is more accessible to aqueous phase. The two recorded DEER traces for spin-labeled mutant N55C and evolution times of 1 μs and 3 μs (Figure 6A) revealed very different form-factors of signal decays. The clearly bimodal character of DEER signal trace for the shorter evolution time (t_m) and the respective distance distribution are shown in Figures 6B and 6C. For the 3 μs data, however, one can see what appears mostly as a

slow “uniform” background with a small narrow feature in the beginning of the record. To produce such signal in a spin pair widely distributed distance above 80 Å would be necessary.[14]

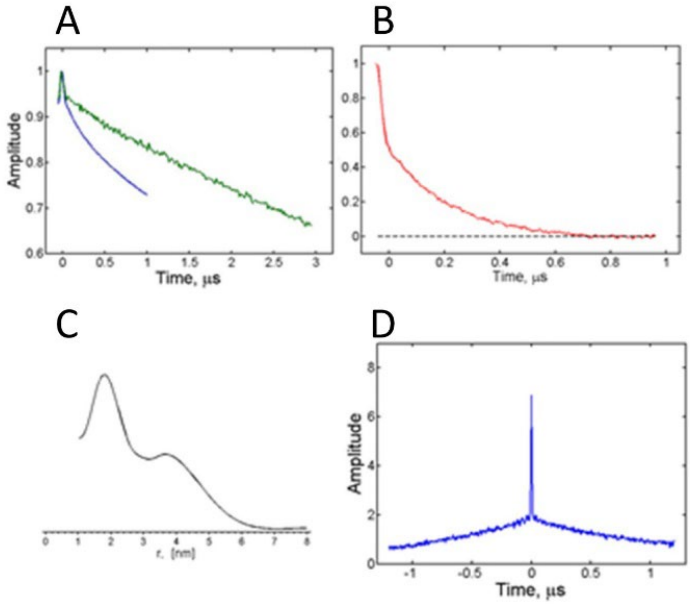

Figure 6. The DEER data and reconstructed inter-spin distances for Vpu spin-labeled at residue N55C. (**A**) Raw DEER data recorded for two different evolution times, 1 µs and 3 µs. (**B**) Background subtracted DEER signal for 1 µs evolution time data in A. (**C**) The reconstructed inter-spin distances for the data in B. (**D**) The intense narrow peak in DQC data originates from very short distances on the order of 10 Å for some spin-labels at N55C in Vpu oligomer. These distances are too short to be sensed by DEER whose sensitivity rolls off quickly below 20 Å.

These observations suggest that spin labels in close proximity or at moderate distances in Figure 6C and Figure 6D have shorter relaxation times than a fraction of labeled sites, which may be located far away from these apparent spin clusters by the nature of the oligomeric assembly. They could be residing on less restricted “floppy” domains, so that only small dipolar evolution occurs on a limited time-scale. For long evolution times these slowly-relaxing spins-labels contribute most of the echo signal and long distances due to these sites dominate the DEER signal. It is unlikely that these slow decays are caused by intermolecular spin interactions since oligomer spin clusters are confined to widely separated complexes. In such cases analogues to spin-labeled micelles, intermolecular contributions to DEER signal are small.[14]

This result suggests that the Vpu region containing the loop between Helices 2 and 3, and possibly Helix 3, are sampling multiple conformations outside the Vpu oligomer core. This is in line with cryoEM results (Figures 3 and 4) indicating that this protein region is not well resolved in the structures.

However, in addition to this broadly distributed distances, for the residue N55C we also observed a measurable contribution of very short inter-spin distances at or below 10 Å reported by double quantum coherence (DQC),[15] as shown in Figure 6D. Apparently, these very short distances correspond to a not yet quantified fraction of labels occupying sites locked in distinct conformations. They possibly contribute broad and difficult to quantify lines in the EPR spectrum of residue N55C in Figure 5B. Based on these results, we may conclude that some of Helices 2 and possibly Helices 3 from different protomers interact with each other and/or the oligomeric core, bringing into proximity the residues N55 in the Vpu oligomer.

This could explain the presence of peripheral low electron densities in the cryo-EM strictures encircled in yellow in Figure 3D.

Conclusions

Vpu is a HIV-1 encoded accessory protein, which has been linked to several processes important for the virus functions in the infected cells.[1d, 1f, 16] However, at present, the Vpu structures underlying these functions are not characterized in sufficient detail. In addition, in cellular membranes, Vpu is thought to function in both oligomeric and monomeric states,[3a] but the factors governing the quaternary structure variations have not been adequately identified and studied. Furthermore, we[5] and others[3d] found that this protein forms soluble oligomers outside of membrane or hydrophobic environment. This is atypical behavior for a transmembrane protein, although other such proteins alternating between soluble and membrane-bound functional states are known.[6-7] It may well be that the observed soluble oligomers of Vpu are purely a result of fortuitous physicochemical properties, as currently there is insufficient evidence to confirm or rule out their physiological relevance. One plausible role could be that soluble oligomers serve a shuttle of this protein between cellular compartments. Despite the insufficient knowledge of their functionality, the soluble Vpu oligomers present an interesting supramolecular construct to study interaction and folding of certain polypeptides, cooperativity, and formation of protein superstructures. This motivates our interest in elucidating their structural properties and the mechanism of assembly. To this end, we applied several experimental techniques that are cryoEM, EPR, SEC and protein engineering. The cryoEM data we obtained were of adequate quality to build a 3-D structural model of MBP-Vpu oligomers and the best fit of this model was obtained for MBP-FL Vpu hexamers, but heptamers cannot be ruled out. We also found that the oligomer formation is a result of Vpu Helix 1 self-association, and Helix 2 has stabilizing effect, as observed by SEC. It is not yet known how the regions of Helices 1 (TMs) are structured in the Vpu oligomer. The CW EPR and DEER data based on the singly spin-labeled residue N55C in Vpu C-terminal domain indicated that this Vpu region is highly dynamic, sampling a wide range of conformations, and the labeled sites at the C-termini of protein protomers are mostly widely separated.

Thus, the results from this and previous studies provided unambiguous evidence that Vpu forms well-defined and stable oligomers in solution. Further studies, some of which are ongoing, would make available more information on the structure of these oligomers and could possibly serve as a ground to uncover a physiological function linked to them.

Based on the results from this study, we propose a model of Vpu soluble oligomers in which the regions of Helices 1 self-associate to form a hydrophobic core of possibly a hexameric quaternary structure, which is further stabilized by the favorable arrangement of amphipathic Helices 2 and linkers between Helix 1 and Helix 2 of each protomer (Figure 7). The linker and Helix 2 of individual protomers might be parted, but it may well be that the negatively charged residue in the linker of one protomer (colored in red in Figure 7) interact electrostatically with some of the residues in the cluster of positively charged amino acids (colored in blue in Figure 7) from the proximal protomers to reinforce oligomer stability. In this case there is high probability for the residue Q36 to be occluded in agreement with CW EPR and DEER.[5] Helices 3 are predominantly spread apart and are highly dynamic.

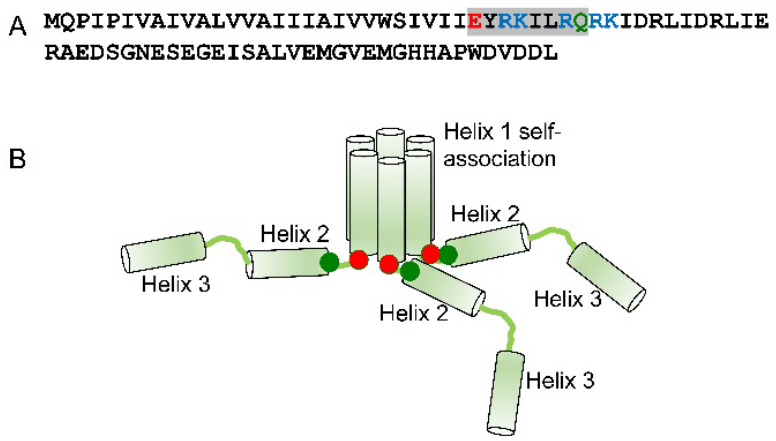

Figure 7. Proposed model of the soluble Vpu oligomers. (A) Amino acid sequence of FL Vpu. The linker between Helix 1 and Helix 2 is highlighted in gray, and the residue Q36 is in green. The negatively charged residue E29 is in red and the cluster of positively charged residues R31, K32 and R35 are in blue. (B) Hexametric arrangement of Vpu monomers: Helices 1 from six protomers come together to form the oligomer core. The linker between Helix 1 and Helix 2, and Helix 2 in each protomer are arranged in a way to stabilize the oligomer. Residue Q36 (dark green circle) is possibly oriented toward the oligomer core and occluded. Helix 3 is widely spread and conformationally heterogeneous. Helices 2 and 3 for only three protomers are shown for clarity.

Acknowledgements

We greatfuly acknowlege Isaac Forrester for collecting the cryo-EM data used in this study. Oluwatosin Adetyui is acknowledged for participation in intial production of MBP-FL Vpu protein. The study was supported by start-up funds from the Department of Chemistry and Biochemistry at TTU (to ERG), NIH grant R01GM080139 (SJL, Baylor College of Medicine), and NIH grant 1R24GM146107 (National Biomedical Resource for Advanced ESR Techniques, ACERT, Cornell University).

Author contribution

SM: experiment, data analysis and interpretation, figures, writing the manuscript; LD: data analysis and interpretation, figures, writing the manuscript; MMI: experiment, data analysis; OI: experiment; PPB: experiment, data analysis and interpretation; figures, writing the manuscript; SJL: supervision, funds acquisition, data interpretation; ERG: conception, design, experiment, data analysis and interpretation, figures, writing the manuscript, supervision, funds acquisition. All authors contributed to and agreed with the final version of the manuscript.

Keywords: Vpu soluble oligomer, cryoEM on soluble Vpu oligomer, cryoEM structure of oligomeric protein, DEER study on soluble Vpu oligomer

Declaration of interests: The authors declare no competing interests.

References

[1] aR. S. Mitchell, C. Katsura, M. A. Skasko, K. Fitzpatrick, D. Lau, A. Ruiz, E. B. Stephens, F. Margottin-Goguet, R. Benarous, J. C. Guatelli, *PLoS Pathog* **2009**, *5*, e1000450; bN. Roy, G. Pacini, C. Berlioz-Torrent, K. Janvier, *Front Microbiol* **2014**, *5*, 177; cK. Strebel, T. Klimkait, M. A. Martin, *Science* **1988**, *241*, 1221-1223; dM. E. Gonzalez, *Viruses* **2015**, *7*, 4352-4368; eN. Khan, J. D. Geiger, *Viruses* **2021**, *13*; fM. Dube, M. G. Bego, C. Paquay, E. A. Cohen, *Retrovirology* **2010**, *7*, 114.

[2] aE. A. Cohen, E. F. Terwilliger, J. G. Sodroski, W. A. Haseltine, *Nature* **1988**, *334*, 532-534; bK. Strebel, T. Klimkait, F. Maldarelli, M. A. Martin, *J Virol* **1989**, *63*, 3784-3791; cP. W. Ramirez, S. Sharma, R. Singh, C. A. Stoneham, T. Vollbrecht, J. Guatelli, *Cells* **2019**, *8*.

[3] aA. Hussain, S. R. Das, C. Tanwar, S. Jameel, *Virol J* **2007**, *4*, 81; bS. Langer, C. Hammer, K. Hopfensperger, L. Klein, D. Hotter, P. D. De Jesus, K. M. Herbert, L. Pache, N. Smith, J. A. van der Merwe, S. K. Chanda, J. Fellay, F. Kirchhoff, D. Sauter, *Elife* **2019**, *8*; cC. Ma, F. M. Marassi, D. H. Jones, S. K. Straus, S. Bour, K. Strebel, U. Schubert, M. Oblatt-Montal, M. Montal, S. J. Opella, *Protein Sci* **2002**, *11*, 546-557; dF. Maldarelli, M. Y. Chen, R. L. Willey, K. Strebel, *J Virol* **1993**, *67*, 5056-5061.

[4] aS. J. Neil, V. Sandrin, W. I. Sundquist, P. D. Bieniasz, *Cell Host Microbe* **2007**, *2*, 193-203; bS. J. Neil, T. Zang, P. D. Bieniasz, *Nature* **2008**, *451*, 425-430.

[5] S. Majeed, O. Adetyui, P. P. Borbat, M. M. Islam, O. Ishola, B. Zhao, E. R. Georgieva, *Journal of Structural Biology* **2023**, *215*, 107943.

[6] Y. T. Hsu, K. G. Wolter, R. J. Youle, *Proc Natl Acad Sci U S A* **1997**, *94*, 3668-3672.

[7] C. Lesieur, B. Vecsey-Semjen, L. Abrami, M. Fivaz, F. Gisou van der Goot, *Mol Membr Biol* **1997**, *14*, 45-64.

[8] V. Cabra, M. Samso, *J Vis Exp* **2015**, 52311.

[9] S. H. Scheres, *J Struct Biol* **2012**, *180*, 519-530.

[10] M. Chen, S. J. Ludtke, *Nat Methods* **2021**, *18*, 930-936.

[11] aR. S. Cooper, E. R. Georgieva, P. P. Borbat, J. H. Freed, E. E. Heldwein, *Nat Struct Mol Biol* **2018**, *25*, 416-424; bE. R. Georgieva, S. Xiao, P. P. Borbat, J. H. Freed, D. Eliezer, *Biophys J* **2014**, *107*, 1441-1452; cE. R. Georgieva, *Nanotechnol Rev* **2017**, *6*, 75-92; dF. Torricella, A. Pierro, E. Mileo, V. Belle, A. Bonucci, *Biochim Biophys Acta Proteins Proteom* **2021**, *1869*, 140653; eH. S. McHaourab, P. R. Steed, K. Kazmier, *Structure* **2011**, *19*, 1549-1561.

[12] aH. Zhang, E. C. Lin, B. B. Das, Y. Tian, S. J. Opella, *Biochim Biophys Acta* **2015**, *1848*, 3007-3018; bD. Willbold, S. Hoffmann, P. Rosch, *Eur J Biochem* **1997**, *245*, 581-588.

[13] aP. P. Borbat, E. R. Georgieva, J. H. Freed, *J Phys Chem Lett* **2013**, *4*, 170-175; bE. R. Georgieva, A. S. Roy, V. M. Grigoryants, P. P. Borbat, K. A. Earle, C. P. Scholes, J. H. Freed, *J Magn Reson* **2012**, *216*, 69-77; cE. R. Georgieva, P. P. Borbat, C. Ginter, J. H. Freed, O. Boudker, *Nat Struct Mol Biol* **2013**, *20*, 215-221.

[14] P. P. Borbat, K. Surendhran, M. Bortolus, P. Zou, J. H. Freed, H. S. McHaourab, *PLoS Biol* **2007**, *5*, e271.

[15] P. P. Borbat, H. S. McHaourab, J. H. Freed, *J Am Chem Soc* **2002**, *124*, 5304-5314.

[16] aJ. L. Douglas, K. Viswanathan, M. N. McCarroll, J. K. Gustin, K. Fruh, A. V. Moses, *J Virol* **2009**, *83*, 7931-7947; bG. D. Ewart, T. Sutherland, P. W. Gage, G. B. Cox, *J Virol* **1996**, *70*, 7108-7115.